J Mater Sci (2018) 53:3106–3118

Biomaterials

Synthesis and characterization of gold-conjugated *Backhousia citriodora* nanoparticles and their anticancer activity against MCF-7 breast and HepG2 liver cancer cell lines

Roshanak Khandanlou[1,*], Vinuthaa Murthy[1], Dhananjaya Saranath[2], and Hetal Damani[2]

[1] School of Psychological and Clinical Sciences, Faculty of Engineering, Health, Science and the Environment, Charles Darwin University, Darwin 0909, Australia

[2] Department of Biological Sciences, Sunandan Divatia School of Science, NMIMS (Deemed to be) University, Mumbai, Maharashtra 400056, India

Received: 21 June 2017
Accepted: 24 October 2017
Published online: 1 November 2017

ABSTRACT

Environmentally benign-synthesized gold nanoparticles (Au-NPs) have received substantial attention owing to their biomedical applications, particularly in cancer therapy. In the current study, *Backhousia citriodora* (*B. citriodora*) leaf extract was applied as a reducing agent for one-pot synthesis of controlled size Au-NPs. The effect of various parameters such as reaction time, pH, and *B. citriodora* leaf boiling time on the synthesis of Au-NPs was studied. The characterization of the Au-NPs synthesized at 15.0-min incubation time showed colour change because of the surface plasma resonance band around 530.0 nm. TEM photographs showed spherical morphologies with an average size of 8.40 ± 0.084 nm and zeta potential value was − 29.74 mV, indicating stability of the nanoparticles. The biomedical properties of Au-NPs and *B. citriodora* leaf extract showed strong DPPH radical scavenging. The in vitro anticancer activity determined using MTT assay exhibited that Au-NPs showed a significant dose-dependent reduction in the viability of the MCF-7 breast cancer cell line and the HepG2 liver cancer cell line with IC_{50} values of 116.65 and 108.21 µg, respectively.

Introduction

Recent advances in nanotechnology have promoted a wide growth in synthesis of nanoparticles in several science fields, including medicine, electronics, and agriculture [1, 2]. Noble metal nanoparticles show distinct properties compared to other metallic nanoparticles due to their optical, electronic and molecular recognition properties. Noble metal nanoparticles have large optical field enhancements

Address correspondence to E-mail: roshanak.khandanlou@cdu.edu.au

https://doi.org/10.1007/s10853-017-1756-4

due to the resonant oscillation of their free electrons in the presence of light. Due to these properties, noble metal nanoparticles are increasingly utilized in imaging, sensors, cosmetics, cancer therapy, and drug delivery systems [3]. Amongst these noble metals, gold nanoparticles are inert and not easily oxidized when exposed to oxygen or a highly acid environment [4]. Gold nanoparticles exhibit different colours, such as red, blue or other colours, depending on their size, shape and amount of aggregation [4, 5]. These visible colours reflect the oscillations of conduction band electrons at appropriate wavelengths [6]. Gold nanoparticles are highly stable, sensitive and have higher levels of consistency. Due to these properties, they are utilized for biomedical applications such as drug delivery, imaging, photothermal therapy and immunochromatographic detection of pathogens in food and clinical specimens [7].

Various physical and chemical methods are traditionally used for synthesis of gold nanoparticles. Surfactants, polymers, starch, dendrimers and lipids are used as stabilizers of metal nanoparticle applications [8]. However, Au-NPs prepared by these methods are unsuitable for medical applications due to the high cost and toxicity of chemicals used as reducing and stabilizing agents [9]. A number of research papers were published in the last decade on plant extract mediated synthesis of metal nanoparticles with shape, size and stability suitable for biological and medical applications [10]. Aqueous plant extracts contain non-toxic and biocompatible phytochemicals that can effectively reduce gold ions to nanoparticles with controllable size and stability [11, 12]. The conjugation of plant ingredients with nanoparticles leads to stabilization of the medium, hindering aggregation in physiological conditions, producing biocompatible functionalities to the nanoparticles for improved biological interactions. Currently, there is a need to develop environmentally benign procedures using plant extracts for the synthesis of NPs, which can potentially increase medical benefits [13, 14].

Backhousia citriodora of the Myrtaceae family, a native to Queensland (Australia) subtropical rainforests, is perhaps the most commercialized native spice currently available, with thousands of trees under cultivation. Polyphenol-rich extracts obtained from the herb contain bioactive flavonoids, phenolic acids and tannins. The compounds possess numerous health-enhancing properties [15].

Cancer is an abnormal growth of tissue or cells exhibiting uncontrolled proliferation autonomously resulting in a progressive increase in the number of cell divisions. It causes significant morbidity and mortality and is a major health problem worldwide [16] which has resulted in increasing demand for anticancer therapy [17]. The fight against cancer is difficult, particularly in the development of therapies for aggressive, rapidly multiplying tumours. Chemotherapy is available for treatment of cancer, but exhibits low specificity and is restricted by dose-limiting toxicity. It is a challenge to find appropriate therapy and drugs for the treatment of various types of cancer with minimal side effects. So, conventional methods require the combination of controlled release technology and targeted drug delivery for increased efficacy and decreased toxicity. Nanomaterials are anticipated to revolutionize cancer diagnosis and therapy [18].

In the current study, we report a novel method of synthesis and characterization of Au-NPs with *B. citriodora* leaf extract. The influence of different parameters, such as reaction time, pH, and boiling time of *B. citriodora* leaf aqueous extract on the synthesis of Au-NPs, was investigated. The anticancer activity of synthesized Au-NPs against the breast cancer cell line MCF-7, the liver cancer cell line HepG2 and human dermal fibroblast cells HDF-7 is also reported. To the best of our knowledge, the *B. citriodora* leaf extract has not been used for preparation of Au-NPs.

Experimental methodology

Gold (III) chloride trihydrate (99.9%) ($HAuCl_4{\cdot}3H_2O$) was purchased from Sigma-Aldrich, USA. 2,2-diphenyl-1-picrylhydrazyl (DPPH) was supplied by Sigma-Aldrich, Germany. The fresh leaves of *B. citriodora* were collected from Charles Darwin University, Australia.

The fresh leaves of *B. citriodora* were washed several times with pure water until no foreign material remained. 5.0 g of leaf was finely cut and stirred with 100.0 mL of high-pure water at 85.0 °C for 3.0 min. The leaf extract was filtered through Whatman No. 1 filter paper, and the filtrate was stored at 4.0 °C for further experiments.

The synthesis of Au-NPs involved mixing of specific amounts of $HAuCl_4{\cdot}3H_2O$ and *B. citriodora*

leaf extract in water. 5.0 ml of 5.0 mM $HAuCl_4$ was added to a vigorously stirred 2.0 mL extract at pH 5.16, and stirring was continued for 2.0 min at room temperature. Rapid reduction took place and was completed in 15.0 min by visual colour change from light yellow to stable violet and then to ruby red colour. Different experimental parameters such as reaction time (5.0, 10.0, 15.0 and 20.0 min), pH (2.03, 4.15, 5.16, 7.18 and 9.10), and boiling time of *B. citriodora* leaf (1.0, 3.0, 5.0 and 7.0 min) were optimized to get the maximum yield of synthesized Au-NPs.

Formation of Au-NPs was confirmed by UV–Vis spectroscopy (Varian, Cary 100) in a range of 200–800 nm. FT-IR spectra was detected via KBr plate for the *B. citriodora* leaf extract and Au-NPs using Perkin-Elmer SP6E ONE. The morphology and size of Au-NPs was measured by TEM, which was conducted using a JEOL 2100 TEM electron microscope equipped with SAED. SEM (JEOL) JSM-7001 Field Emission SEM equipped with Oxford Instruments X-Max detector for EDS analysis was used to examine the morphology and elemental composition of the samples. The crystalline nature of the Au-NPs was assessed by X-ray diffraction method using Rigaku SmartLab diffractometer (Cu source, 40 kV 40 mA) at a step size of 0.04° at 1.5° min^{-1}. A surface charge of synthesized Au-NPs was analysed using a zeta potential analyser (NICOMP™ 380 ZLS).

The free radical scavenging activity was analysed through ability of the nanoparticles to scavenge free radicals. DPPH generates a free radical which is extensively used to screen the ability of different antioxidants to scavenge the free radical (electron donating capability of a compound). Due to the presence of an unpaired electron, DPPH has a dark violet colour. The radical scavenging was monitored using UV–Vis spectroscopy as reduction of absorbance intensity at 517.0 nm, where the colour alters from violet free radical to pale yellow non-radical form [19].

Aliquots (1.0 mL) of different volume of *B. citriodora* leaf extract and Au-NPs [5.0 (0.35, 0.09 μg/μL), 10.0 (0.71, 0.17 μg/μL), 15.0 (1.07, 0.26 μg/μL), 20.0 (1.42, 0.35 μg/μL), 25.0 (1.78, 0.446 μg/μL), and 50.0 μL (3.57, 0.92 μg/μL)], respectively, in methanol were added to 1.0 mL, 1.0 mM methanolic solution of DPPH. After 30.0 min at room temperature, absorbance was read against blank samples at 517.0 nm using UV–Vis spectrophotometer. Percentage inhibition of DPPH oxidation was calculated using the following Eq. (1).

$$\text{DPPH scavenging effect}\% = \left[\frac{A_{\text{control}} - A_{\text{sample}}}{A_{\text{control}}}\right] \times 100, \quad (1)$$

where A_{control} is the absorbance of the DPPH solution and A_{sample} is the absorbance of the test sample.

The human breast cancer MCF-7 cell line and the liver cancer HepG2 cell line were purchased from the National Centre for Cell Sciences (NCCS) (Pune, India), and the human dermal fibroblast HDF-7 cells were purchased from American Type Culture Collection (ATCC) (Maryland, USA). The cells were grown in Dulbecco's Modified Eagle's Medium (DMEM) (CELLclone, India) supplemented with 1.0 mM sodium pyruvate, 2.0 mM L-glutamine, 10.0% foetal bovine serum (FBS) (GIBCO, India), and a mixture of 10.0 mg/mL streptomycin, 10000 units/mL penicillin, and 25.0 μg/mL amphotericin B (Sigma-Aldrich, USA), and then incubated at 37.0 °C in a humidified atmosphere containing 5.0% CO_2. An MTT (3-(4,5-dimethylthiazol-2-yl)-2,5-diphenyltetrazolium bromide) (Himedia, France) assay was carried out to study the cytotoxic effects of the Au-NPs and *B. citriodora* leaf extract on the MCF-7 cells, HepG2 cells, and human dermal fibroblast HDF-7 normal cells. Cells were seeded into 96-well plates at about 10000 cells/well and incubated for 24 h at 37.0 °C. The cells were treated with different concentrations of BCAu-NPs and *B. citriodora* leaf extracts (50.0, 100.0, 150.0, 200.0, 250.0, and 500.0 and 1000.0 μg) and incubated for 24 h at 37 °C. To minimize the effect of colour of the extract and BCAu-NPs on the absorbance value, the medium containing the extract and BCAu-NPs was removed. Further, the wells were washed with warm DPBS to ensure removal of traces of the coloured extract and 100.0 μL MTT (0.5 mg/mL) was added to each of the wells and the plate was incubated at 37.0 °C for 4.0 h. The formed purple colour formazan crystal was dissolved by addition of 150 μL DMSO in each well. Absorbance was recorded after 15.0 min at 570.0 nm against a reference wavelength of 655.0 nm using a Bio-Rad 680 microplate reader, and the standard curves of cell number from the optical density (OD) were utilized to determine the percentage of cell viability. The cell viability is calculated as Eq. (2):

$$\text{Cell viability}\% = \frac{\text{OD of treated cells}}{\text{OD of untreated cells}} \times 100 \qquad (2)$$

In addition, the inhibitory concentrations (IC_{50}) of BCAu-NPs and *B. citriodora* leaf extract against the MCF-7, HepG2, and HDF-7 cells were calculated at 24 h on addition of BCAu-NPs and *B. citriodora* leaf extract.

The statistical analysis was performed in GraphPad Prism 5 (GraphPad Software, CA, USA). Two-way analysis of variance (ANOVA) was used to analyse the data sets, with Bonferroni post hoc tests to compare the cytotoxic effects of *B. citriodora* leaf extract, BCAu-NPs, and doxorubicin and also the antioxidant activities of *B. citriodora* leaf extract and the BCAu-NPs. Bars in columns are presented as mean ± standard error of mean (SEM), and *P* values < 0.001 and < 0.05 are considered as significant for antioxidant activity and cytotoxic effect of *B. citriodora* leaf extract and BCAu-NPs, respectively.

Results and discussion

Synthesis and characterization of gold-conjugated *B. citriodora* nanoparticles

In the current research, synthesis of Au-NPs from *B. citriodora* leaf extract occurred rapidly at room temperature and at pH 5.16, the reaction completed within 15.0 min and there was no subsequent colour change. Reduction in Au^{3+} to Au^{0} is marked by the colour change of the solution from pale yellow to ruby red (Fig. 1). In the synthesis of Au-NPs, the interactions between *B. citriodora* leaf ingredients and gold particles occurred directly and no other chemical or artificial reagents were required.

The impact of pH was assessed over a range of pH 2.0–9.0. The maximum yield of Au-NPs was acquired at pH 5.16. Figure 2a represents the influence of the pH on the formation of Au-NPs. As shown in the figure, the absorbance increases with increasing pH up to 5.16 with a blue shift in the wavelength. The effective synthesis of Au-NPs at lower or acidic pH is in agreement with the obtained results by Sathishkumar et al. [20] where the synthesis of Au-NPs via star anise was optimized at pH 4.0. As shown in Fig. 2a, the preparation of Au-NPs at pH 2.0 was very weak and negligible. Degradation or inactivation of bioactive molecules at this high-acidic pH can be caused due to insignificant synthesis of Au-NPs. The UV–Vis spectra analysis revealed increasing pH beyond 5.16 resulted in a decline in the peak/absorbance intensity. A feasible reason for this phenomenon during increasing pH could be the change in positive net charge to negative on the biomolecules, leading to intense repulsion between the biomolecules and the $AuCl_4^-$ ions which are negatively charged [21]. The presence of bigger nanoparticles at extreme acidic pH could be ascribed to the uncontrolled nucleation and aggregation owing to superior interaction of $AuCl_4^-$ ions [3]. Thus, pH 5.16 was considered as optimum for the Au-NPs synthesis using the leaf extract of *B. citriodora*.

The UV–Vis spectra recorded from the *B. citriodora* leaf extract, with gold ion reaction mixture, at different reaction times (5.0, 10.0, 15.0 and 20.0 min), are plotted in Fig. 2b. The spectra show a well-defined surface plasmon band centred at around 530.0 nm for Au-NPs. It can be seen that with the increase in

Figure 1 Schematic illustration of the colour change after the addition of chloroauric acid **a** *B. citriodora* leaf extract, and **b** Au-NPs colloidal solution after the reaction.

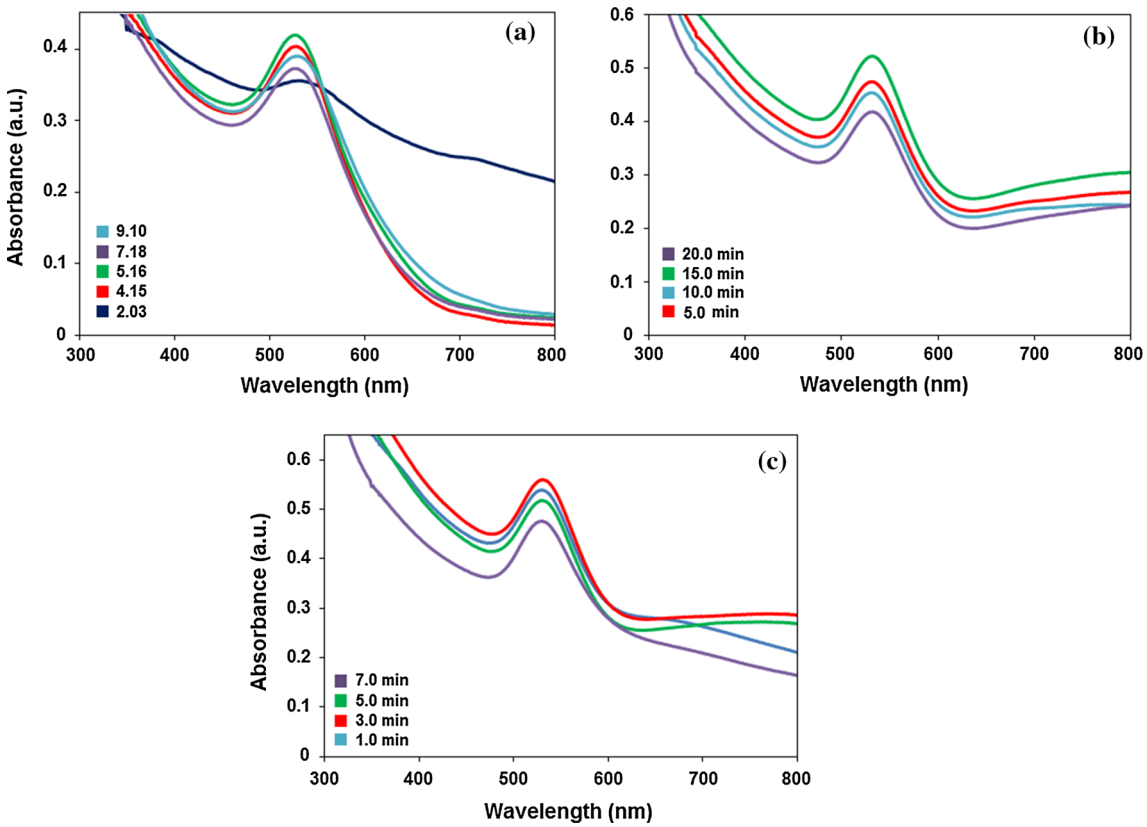

Figure 2 UV–visible spectra of Au-NPs prepared at different **a** pH, **b** reaction time, and **c** *B. citriodora* leaf boiling time.

reaction time, the intensity of peaks is raised and shifted to the lower wavelength up to 15.0 min. Beyond 15.0 min, the peaks show red shift. In addition, the colour intensity of gold is raised with increasing the incubation time and it reveals the formation of an increased number of nanoparticles.

Reducing equivalents such as phenolic acids as an active ingredient are required for the preparation of Au-NPs from biological extracts [22]. The active chemical ingredients could reduce the metal ion to its non-ionic type and leads to its reduction throughout the procedure. The extraction conditions, chemical nature, and the particle size of the sample could have affected extraction of the active ingredients from plant sources [20, 23]. Amongst all the conditions, extraction length and temperature are identified as significant parameters which should be optimized [24]. In the current research, extraction was done at a high temperature in a short period of time. Hence, the temperature was kept consistent at 85.0 °C, and optimization of the extraction length was done through boiling of *B. citriodora* leaves at various times (1.0, 3.0, 5.0 and 7.0 min) and analysed as for Au-NPs preparation using UV–Vis spectrum. The Au-NPs yield exhibited the following pattern: 7.0 min < 5.0 - min < 1.0 min < 3.0 min (Fig. 2c). At 1.0 min, it is possible that all the active ingredients did not solubilize, resulting in insignificant Au-NPs yield. At longer boiling time (5.0 and 7.0 min), the phenolic ingredients can be denatured. It is also feasible that phenolics oxidized at higher boiling times [20]. Due to the direct dependency of Au-NPs yield on the quantity of reducing equivalents, the maximum yield was found at 3.0 min. The optimized parameters of Au-NPs are shown in Table 1.

After optimization, Au-NPs were synthesized at pH 5.16 with reaction time of 15.0 min by using the *B. citriodora* leaf extract of 3.0-min boiling time.

XRD analysis affirmed the crystalline nature of Au-NPs. Figure 3a indicates that the obtained XRD pattern through reduction in Au^{3+} ions to Au^{0} has crystalline structure. The diffraction pattern of Au-NPs shows intense bands at $2\theta = 38.32°$, 44.56°, 64.96°, and 78.04° which could be ascribed to (111), (200), (220), and (311) reflections which represents the face-centred cubic (fcc) structure of Au-NPs which

Table 1 Optimized parameters of Au-NPs

	pH	Reaction time (min)	*B.citriodora* leaf boiling time (min)
Au-NPs optimization	5.16	15.0	3.0

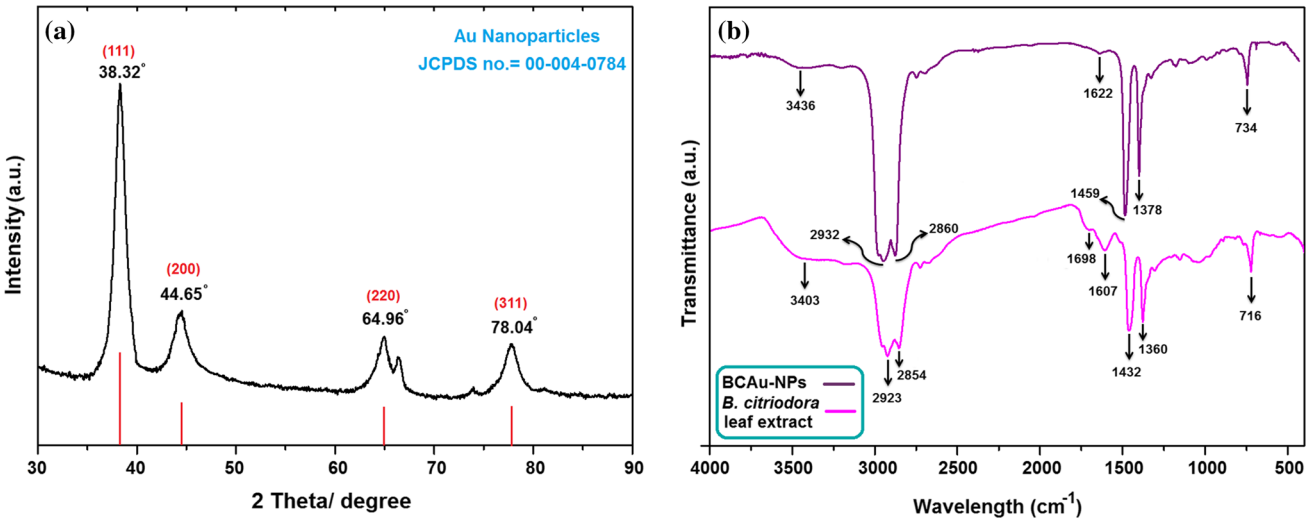

Figure 3 **a** XRD pattern of purified Au-NPs synthesized using *B. citriodora* leaf extract, **b** FT-IR spectra of *B. citriodora* leaf extract and synthesized Au-NPs.

are distinguished with (JCPDS No. 00-004-0784) [25]. This result revealed the pure crystalline gold composition of Au-NPs. The Debye–Scherrer equation was used to determine the average crystallite size (d).

$$d = K\lambda/\beta_{\frac{1}{2}}\cos\theta, \quad (3)$$

where K (0.9) is Scherrer's constant, λ (1.5418 Å) is the wavelength, $\beta_{1/2}$ is the peak width at half height, and θ is the Bragg's angle. According to Eq. (3), the average crystallite size of Au-NPs was around 9.0 nm which agreed with the TEM result discussed later.

FT-IR analysis was conducted to detect the presence of possible biomolecules in *B. citriodora* leaf extract responsible for capping, which leads to efficient stabilization of Au-NPs. The FT-IR spectrum of *B. citriodora* leaf extract (Fig. 3b) showed a band at 3403 cm^{-1} corresponding to hydroxyl functional group of polyphenolic compounds or N–H of amines. The bands at 2923 and 2854 cm^{-1} correspond to asymmetric stretching of C–H groups. The bands at 1698 and 1607 cm^{-1} indicated the presence of chelated carbonyl functional groups of carboxylic acid or amide. The peaks at 1432 and 1360 cm^{-1} are due to C=C stretching [26]. The minor peak at 727 cm^{-1} can be due to the leaching of Cl^- ions from $HAuCl_4$ [27, 28]. The FT-IR spectrum of Au-NPs (Fig. 3b) revealed a slight shift, reduction, and absence in band intensity in the N–H or O–H stretching band from 3403 to 3436 cm^{-1}, C–H band from 2923 to 2932 cm^{-1}, C=O stretching from 1607 to 1622 cm^{-1}, respectively. Various reports have been published regarding the role of the carbonyl and hydroxyl groups in carbohydrates, terpenoids, flavonoids, and phenolic compounds as capping, reducing, and stabilizing agents for the preparation of different nanoparticles [29]. In the present study, FT-IR spectrum confirmed the presence of aromatic amines and alcohols which are responsible for the bioreduction in Au^{3+} ions to Au^0 nanoparticles and avoid the agglomeration and cause stabilization of nanoparticles in the medium. Therefore, the *B. citriodora* leaf ingredients act as surfactants and bioreductants.

Figure 4 presents the TEM image and computed histogram of Au-NPs. The TEM analysis revealed that the synthesized Au-NPs are well dispersed and most of the particles are spherical or near spherically shaped ranging from 3.56 to 24.5 nm in size with an average size of 8.40 ± 0.084 nm (Fig. 4a, b, d). Some nanoparticles with triangular, hexagonal, and irregular shapes were also observed. The difference in size and shape of nanoparticles is due to the different growth phases of particles [7]. Further, the SAED pattern confirmed the crystalline structure of the Au-NPs via bright circular spots which can be attributed

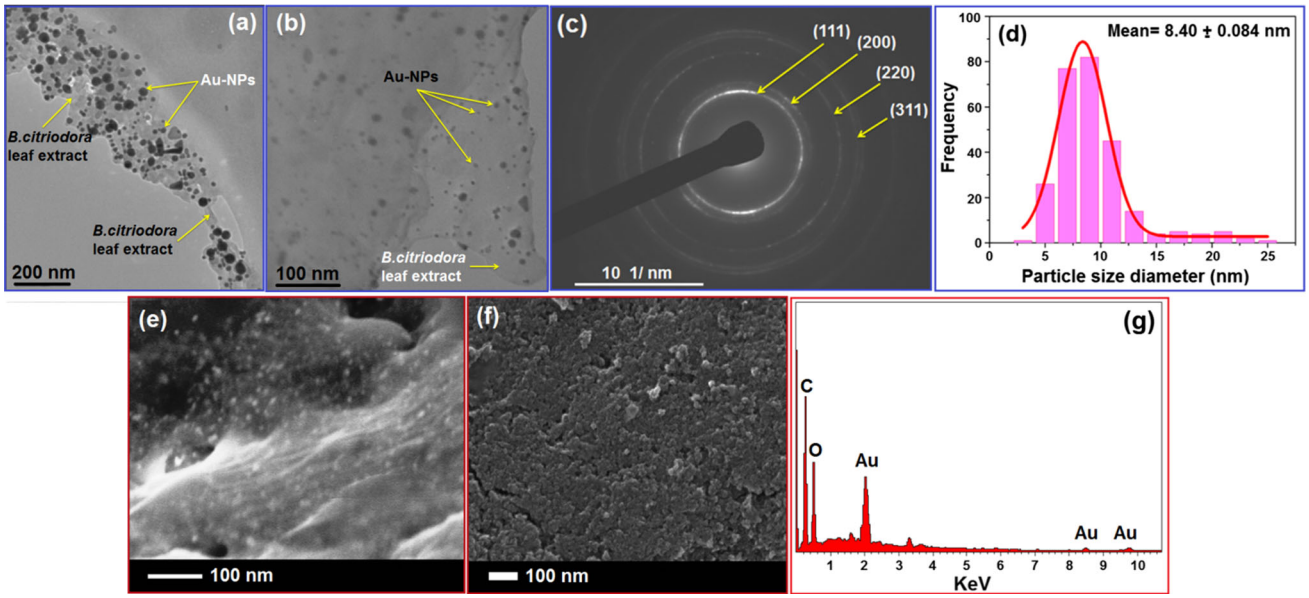

Figure 4 Microscopic images of green-synthesized Au-NPs **a**, **b** TEM micrograph at different magnifications, **c** SAED pattern, **d** particle-size distribution of Au-NPs synthesized from *B. citriodora* leaf extract, **e**, **f** FESEM images at different magnifications, and **g** EDX spectroscopy of Au-NPs synthesized from *B. citriodora* leaf extract.

to (111), (200), (220), and (311) planes of the fcc lattice of Au-NPs (Fig. 4c).

The morphologies of the Au-NPs surfaces were examined by SEM (Fig. 4e, f). The SEM micrographs indicate the formation of spherical nanoparticles which agreed with the TEM images. The presence of gold was confirmed by EDX analysis (Fig. 4g). The existence of gold signal at the spectrum of 2.0 keV was representative of Au-NPs [20]. Oxygen peaks may occur in the spectra because of the bonding of the biomolecules to the surface of Au-NPs positioned at 0.4 keV [30].

The stability of nanoparticles is important when these products are used in biomedical applications [31]. Zeta potential gives the information about the nanoparticles' surface charge and stability. Nanoparticles with zeta potentials higher than 20.0 mV or less than − 20.0 mV have strong electrostatic repulsion and thus remain stable in solution [32]. The zeta potential of the Au-NPs synthesized with *B. citriodora* leaf extract in water is − 29.74 mV which corresponds to the negatively charged Au-NPs (Table 2). A high negative zeta potential corresponds to the repulsive interaction between nanoparticles aimed at preventing the agglomeration of Au-NPs, thus exhibiting excellent stability without a significant increase in size during the incubation period in water. The negative surface charge of Au-NPs

Table 2 Zeta potential of gold-conjugated *B. citriodora* nanoparticles

	Zeta potential (mV)	Mobility (M.U)	Phase (rad/s)
Au-NPs	− 29.74	− 2.22	62.22

suspensions not only indicates high stability, but also suggests less toxicity to normal cells [33].

Total *B. citriodora* leaf extract polyphenols possess superior antioxidant activities [34, 35]. Consequently, the synthesized Au-NPs were assessed to determine whether they retained the antioxidant properties of *B. citriodora* leaf extract by exploring their DPPH free radical scavenging capacity. The antioxidant properties of the Au-NPs and *B. citriodora* leaf extract were evaluated spectrophotometrically from their ability to convert the violet colour of DPPH into a pale yellow colour. The DPPH scavenging activity of the Au-NPs and *B. citriodora* leaf extract was found to increase with increasing concentration.

To elucidate the statistical significance of the antioxidant activity differences detected for the prepared BCAu-NPs and *B. citriodora* leaf extract, the DPPH scavenging effects at different concentrations were assessed using the analysis of variance (ANOVA). The significance of the correlation is confirmed by the smallest value of Prob > *F* or less than 0.05. The result indicates that the *P* value for both

BCAu-NPs and *B. citriodora* leaf extract is less than 0.05 (P value < 0.001), which demonstrates that the correlation is regarded as being statistically significant.

These results suggest that the higher DPPH antioxidant activities are correlated to the high volume of BCAu-NPs and *B. citriodora* leaf extract which are high in polyphenol content.

The average percentage inhibition was from 15.35 to 62.18% for Au-NPs and 37.78 to 79.35% for *B. citriodora* leaf extract with volume from 5.0 to 50.0 µL, as shown in Fig. 5a. These results support the in vitro antioxidant potential of the BCAu-NPs.

The cytotoxicity of various concentrations of *B. citriodora* leaf extract and BCAu-NPs against MCF-7, HepG2 cancer cell lines, and HDF-7 normal cells after 24 h incubation is shown in Fig. 5b–d. The results of all cytotoxicity assays suggest that BCAu-NPs inhibited potential growth of cancer cells in a dose-dependent manner. The percentage of viability of *B. citriodora* leaf extract treated cells was more than BCAu-NPs treated cells at similar dosages.

Figure 5b, c shows a significant cytotoxic effect starting to emerge at 150.0 µg of BCAu-NPs and *B. citriodora* leaf extract on both MCF-7 and HepG2 cancer cell lines treated for 24 h. MCF-7 cells treated with a dosage of 500.0 µg BCAu-NPs and *B. citriodora*

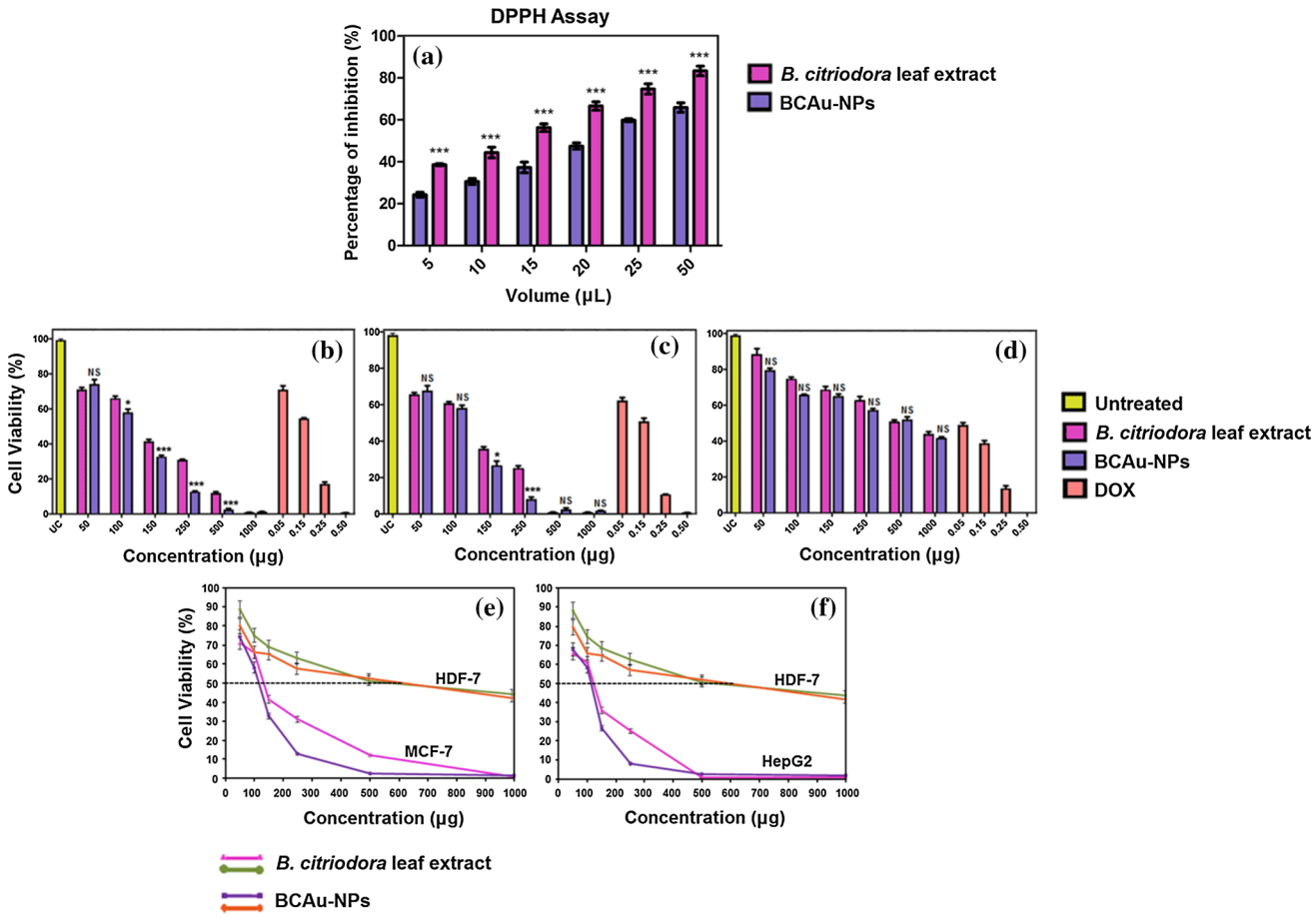

Figure 5 **a** Antioxidant activity of synthesized BCAu-NPs, and *B. citriodora* leaf extract, cytotoxic effect of *B. citriodora* leaf extract and BCAu-NPs on **b** MCF-7, **c** HepG2 cancer cells and **d** HDF-7 normal cells by MTT assay after 24 h, and inhibitory concentration (IC_{50}) of *B. citriodora* leaf extract and BCAu-NPs on **e** MCF-7 cancer, HDF-7 normal cells and **f** HepG2 cancer, HDF-7 normal cells. The results of antioxidant activity and cytotoxic effects were analysed using two-way ANOVA with Bonferroni post hoc test in GraphPad Prism 5: (***indicates significant increase in scavenging effect with *B. citriodora* leaf extract as compared to BCAu-NPs with $p < 0.001$. *Indicates significant increase in cytotoxicity of BCAu-NPs as compared to *B. citriodora* leaf extract with $p < 0.05$. *Significant difference with $p < 0.05$, **significant difference with $p < 0.01$, ***significant difference with $p < 0.001$, *NS* non-significant).

leaf extract for 24 h resulted in 97.4 and 87.9% inhibition of cell proliferation, respectively. HepG2 cancer cell lines treated at half the concentration (i.e. 250 μg) of BCAu-NPs and *B. citriodora* leaf extract resulted in 91.7 and 74.4% inhibition of cell proliferation, respectively.

Both BCAu-NPs and *B. citriodora* leaf extract showed greater than 97.4% inhibition in cell proliferation on HepG2 cancer cells at and above 500.0 μg, but the differences between *B. citriodora* leaf extract and BCAu-NPs inhibitory activity at these levels were non-significant. Besides, no significant toxicity was observed in normal HDF-7 cells treated with *B. citriodora* leaf extract and BCAu-NPs, confirming that *B. citriodora* leaf extract and BCAu-NPs do not affect the viability of normal cells, but rather exhibit a biocompatible nature with normal cells, and therefore are preferred for various biological applications (Fig. 5d) [28].

The observed IC_{50} concentration of BCAu-NPs is used for further investigations. The IC_{50} values of *B. citriodora* leaf extract and BCAu-NPs in MCF-7 and HepG2 cancer cells and HDF-7 normal cells are shown in Fig. 5e, f. As Fig. 5e, f shows, the IC_{50} values of BCAu-NPs were 116.65 and 108.21 μg in MCF-7 and HepG2 cancer cells, respectively. The *B. citriodora* leaf extract exhibited higher IC_{50} values against MCF-7 and HepG2 cancer cells at 136.98 and 117.83 μg, respectively, after 24 h of incubation. The IC_{50} values of *B. citriodora* leaf extract and BCAu-NPs in HDF-7 normal cells were 555.0 and 612.0 μg, respectively (Fig. 5e, f). Results clearly reveal that the BCAu-NPs exhibited selective cytotoxicity against MCF-7 and HepG2 cancer cells, as opposed to the normal HDF-7 cells. An earlier report suggests that the Au-NPs can be used in the destruction of cancer cells and act as potential therapeutic agents [36].

It is also evident that the plant extract shows cytotoxicity against MCF-7 and HepG2 cancer cells and the cytotoxicity of BCAu-NPs is enhanced as the concentration increases, reaching a maximum of 2.5 times and 3.0 times for MCF-7 and HepG2 cancer cells, respectively, compared to that of the plant extract at 250 μg. Thus, we propose that the cytotoxicity is due to the synergistic role of Au-NPs and the plant extract.

To the best of our knowledge, previous studies related to the cytotoxicity of biosynthesized Au-NPs with *B. citriodora* leaf extract against MCF-7 and HepG2 cancer cells have not been reported. From our experimental observations, this report proposes the potential use of synthesized BCAu-NPs in killing MCF-7 and HepG2 cancer cells and may in future lead to development of nanomaterial-based interventions for treatment of the same.

Backhousia citriodora leaf extract-synthesized Au-NPs exhibited substantial cytotoxicity in MCF-7 and HepG2 cells that could be attributed to the synergistic effects of biomolecules such as phenols, alkaloids, and flavonoids assumed to have anti-proliferative activities capped on the BCAu-NPs [37]. Patra et al. [38] found that citrate Au-NPs induced apoptotic death response in a human lung carcinoma cell line (A549), but not on HepG2 cell lines. Connor et al. [39] elucidated that 4.0- and 18.0-nm citrate-bound Au-NPs did not induce cytotoxicity, whereas CTAB (cetyltrimethylammonium bromide)-bound Au-NPs showed significant cytotoxicity. However, CTAB alone also indicated comparable toxicity, demonstrating that Au-NPs are themselves not toxic. Similar studies also proved that bound CTAB is less toxic compared to free CTAB and the free CTAB induced cytotoxicity in human colon carcinoma cells [40]. Hence, based on the results obtained from our in vitro studies, it is evident that bioconjugated Au-NPs synthesized using *B. citriodora* leaf extract have better therapeutic potential compared to chemically synthesized nanoparticles.

Chithrani et al. [41] investigated cellular toxicity of Au-NPs and concluded that Au-NPs enter cells in a shape- and size-dependent manner. Smaller particles have greater surface area to volume ratio and their biological and chemical activity is higher. Due to the large surface area, they adsorb on the macromolecules they encounter and specific cell targeting is achieved due to surface functionalization of Au-NPs [37]. The NPs suppress cell viability by different mechanisms, such as apoptosis and necrosis [42]. Au-NPs at high doses lead to necrosis and at lower doses show apoptosis [43]. Apoptosis is a cell suicide mechanism that controls cell numbers. The apoptotic cascade can be triggered through extrinsic and intrinsic pathways [44]. The induction of tumour cell apoptosis is a crucial mechanism for an anticancer compound. The apoptosis process is characterized by morphological and biochemical changes, and apoptosis of different cells in the same tissue does not occur at the same time [45]. The biofunctionalized Au-NPs are taken into the cells through the process of endocytosis dependent on various properties of

the Au-NPs. In this study, apoptotic and cytotoxic activities could be attributed to the synergistic effect of the Au-NPs functionalized with *B. citriodora* water-soluble phenolic moieties [37].

Nanoparticles could have many adverse effects at the cellular level by interacting with vital cell components such as the membrane, mitochondria, or nucleus. Adverse outcomes could include organelle or DNA damage, oxidative stress, apoptosis (programmed cell death), mutagenesis, and protein up/down regulation [46]. For Au-NPs to be effective as a pharmaceutical, it is essential to have a firm understanding of their biodistribution/accumulation in living systems. The biodistribution of drug carriers is often affected by the route of administration. Nanoparticles used as drug carriers tend to have a longer retention time, generally in the local lymph node, compared to the free drug when administered subcutaneously, intramuscularly, or topically. However, the biodistribution of the nanoparticles largely depends on their surface charge and hydrodynamic radius [47]. In work done by Sonavane et al. [48], particle size was deemed to be important for in vivo permeation. They injected mice with Au-NPs with diameters of 15.0, 50.0, 100.0, and 200.0 nm. After ICP analysis of the various organs and blood, it was revealed that the majority of the gold was present in the liver, lung, and spleen. The 15.0-nm particle seemed to have accumulated the most in all the tissues including blood, liver, lung, spleen, kidney, brain, heart, and stomach. Also, it was discovered that the 15.0 and 50.0 nm were able to cross the blood–brain barrier, whereas the 200.0-nm particle showed a very minute presence in the organs, including blood, brain, stomach, and pancreas.

Accumulation of nanomaterials in the liver and spleen after being taken up by the reticuloendothelial system (part of the immune system with complex components that communicate to identify, capture, and filter foreign antigens and particulates) could lead to hepatic and splenic toxicity [49]. Cho et al. [50] studied the toxicity of 13.0 nm poly (ethylene glycol) (PEG)-modified Au-NPs in mice and found that the nanoparticles accumulate in the liver after injection and induce acute inflammation and cellular damage in the mouse liver.

Injecting Au-NPs in the blood could cause either blood clotting or haemolysis (blood cells break open and release their haemoglobin). Encouragingly, citrate-capped Au-NPs (spheres of diameter 30 and 50 nm) have been shown to be 'blood compatible' and did not induce any detectable platelet aggregation, change in plasma coagulation time, or immune response [51]. Because the size range of nanoparticles matches that of proteins or even small viruses, one might expect that the immune system might react strongly to the presence of nanoparticles in the body, resulting in induced immunotoxicity. The physical and chemical properties of nanoparticles can affect their pharmacokinetics, such as absorption, metabolism, distribution, and elimination. These findings highlight the size-dependent biodistribution of Au-NPs. According to FDA guidelines, pharmaceutical drugs should be eliminated via metabolism or excretion processes after they enter the body. Drug elimination reduces toxicity and prevents drug accumulation. Similar to pharmaceutical drugs, nanoparticles should be designed to be eliminated by the body. Indeed, nanoparticle elimination should be considered seriously, since nanoparticles are more resistant to elimination routes such as metabolism and renal excretion [46]. In one related example, injected semiconductor quantum dots in mice remained intact for more than 2.0 years in mouse tissues, retaining their fluorescence activity. This resistance might be because of their large size (too large to be filtered from the kidney) and their higher chemical stability (against dissolution and degradation) compared to molecules [46].

Conclusion

In the current study, a novel and green method for the synthesis of stable colloidal Au-NPs using *B. citriodora* leaf extract was successfully developed for the first time. The size of Au-NPs was optimized by changing the reaction time, pH, and boiling time of *B. citriodora* leaf. Following the optimization process, maximum yield of synthesized Au-NPs was obtained at an acidic pH of 5.16 at room temperature and the synthesis was completed in 15.0 min. The size, morphology, chemical composition, and surface charge of Au-NPs were assessed through UV–Vis, XRD, TEM, SAED, SEM, EDX, zeta potential, and FT-IR. The synthesized Au-NPs showed spherical or near spherical shape with an average size of 8.40 ± 0.084 nm. XRD and SAED indicated the crystalline nature of prepared Au-NPs. High value of zeta potential (-29.74 mV) confirmed the stability of Au-

NPs. FT-IR analysis affirmed the presence of polyphenolic groups responsible for reduction in $AuCl_4^-$ to Au-NPs. BCAu-NPs showed strong DPPH free radical scavenging activity; hence, the synthesized Au-NPs retained the antioxidant properties of *B. citriodora* leaf extract. The enhanced antioxidant properties were detected for BCAu-NPs and *B. citriodora* leaf extract, and this correlates well with the high content of *B. citriodora* leaf extract which is rich in polyphenols.

In vitro anticancer results indicated that BCAu-NPs induced significant cytotoxicity against MCF-7 and HepG2 cancer cells in a dose-dependent manner and with no significant cytotoxicity on normal HDF-7 cells. The cytotoxic effect of BCAu-NPs might be due to the synergistic action of the phenolic moieties as well as the Au-NPs. It may be valuable to explore biosynthesized Au-NPs as a possible source of novel anticancer drugs.

Acknowledgements

The authors would like to thank the Charles Darwin University for its financial support (faculty research Grant), the Central Analytical Research Facility (CARF) operated by the Institute for Future Environments, Queensland University of Technology (QUT) for SEM, TEM, and XRD facilities and Dr. Sivanesan Arumugam at the Future Industries Institute (FII), University of South Australia, for assistance with obtaining zeta potential values in this research.

Compliance with ethical standards

Conflict of interest The authors declare that they have no conflict of interest.

References

[1] Soundarrajan C, Sankari A, Dhandapani P, Maruthamuthu S, Ravichandran S, Sozhan G, Palaniswamy N (2012) Rapid biological synthesis of platinum nanoparticles using *Ocimum sanctum* for water electrolysis applications. Bioprocess Biosyst Eng 35(5):827–833

[2] Hoshyar R, Khayati GR, Poorgholami M, Kaykhaii M (2016) A novel green one-step synthesis of gold nanoparticles using crocin and their anti-cancer activities. J Photochem Photobiol B 159:237–242

[3] Shankar SS, Rai A, Ahmad A, Sastry M (2004) Rapid synthesis of Au, Ag, and bimetallic Au core–Ag shell nanoparticles using Neem (*Azadirachta indica*) leaf broth. J Colloid Interface Sci 275(2):496–502

[4] Daniel M-C, Astruc D (2004) Gold nanoparticles: assembly, supramolecular chemistry, quantum-size-related properties, and applications toward biology, catalysis, and nanotechnology. Chem Rev 104(1):293–346

[5] Dash SS, Bag BG (2014) Synthesis of gold nanoparticles using renewable *Punica granatum* juice and study of its catalytic activity. Appl Nanosci 4(1):55–59

[6] Murphy CJ, Gole AM, Stone JW, Sisco PN, Alkilany AM, Goldsmith EC, Baxter SC (2008) Gold nanoparticles in biology: beyond toxicity to cellular imaging. Acc Chem Res 41(12):1721–1730

[7] Rajeshkumar S (2016) Anticancer activity of eco-friendly gold nanoparticles against lung and liver cancer cells. J Genet Eng Biotechnol 14:195–202

[8] Khan Z, Bashir O, Hussain JI, Kumar S, Ahmad R (2012) Effects of ionic surfactants on the morphology of silver nanoparticles using Paan (*Piper betel*) leaf petiole extract. Colloids Surf B 98:85–90

[9] Khademi-Azandehi P, Moghaddam J (2015) Green synthesis, characterization and physiological stability of gold nanoparticles from *Stachys lavandulifolia* Vahl extract. Particuology 19:22–26

[10] Kharissova OV, Dias HR, Kharisov BI, Pérez BO, Pérez VMJ (2013) The greener synthesis of nanoparticles. Trends Biotechnol 31(4):240–248

[11] Santra TS, Tseng F-G, Barik TK (2014) Green biosynthesis of gold nanoparticles and biomedical applications. Am J Nano Res Appl 2(6–2):5–12

[12] Irfan M, Ahmad T, Moniruzzaman MM, Abdullah BB, Bhattacharjee S (2016) Ionic liquid mediated biosynthesis of gold nanoparticles using *Elaeis guineensis* (oil palm) leaves extract. Procedia Eng 148:568–572

[13] Gan PP, Li SFY (2012) Potential of plant as a biological factory to synthesize gold and silver nanoparticles and their applications. Rev Environ Sci Biotechnol 11(2):169–206

[14] Dorosti N, Jamshidi F (2016) Plant-mediated gold nanoparticles by *Dracocephalum kotschyi* as anticholinesterase agent: synthesis, characterization, and evaluation of anticancer and antibacterial activity. J Appl Biomed 14:235–245

[15] Guo Y, Sakulnarmrat K, Konczak I (2014) Anti-inflammatory potential of native Australian herbs polyphenols. Toxicol Rep 1:385–390

[16] Devi JS, Bhimba BV (2012) Silver nanoparticles: antibacterial activity against wound isolates & invitro cytotoxic

activity on Human Caucasian colon adenocarcinoma. Asian Pac J Trop Dis 2:S87–S93

[17] Unno Y, Shino Y, Kondo F, Igarashi N, Wang G, Shimura R, Yamaguchi T, Asano T, Saisho H, Sekiya S (2005) Oncolytic viral therapy for cervical and ovarian cancer cells by Sindbis virus AR339 strain. Clin Cancer Res 11(12):4553–4560

[18] Rosarin FS, Arulmozhi V, Nagarajan S, Mirunalini S (2013) Antiproliferative effect of silver nanoparticles synthesized using amla on Hep2 cell line. Asian Pac J Trop Med 6(1):1–10

[19] Mukherjee S, Ghosh S, Das DK, Chakraborty P, Choudhury S, Gupta P, Adhikary A, Dey S, Chattopadhyay S (2015) Gold-conjugated green tea nanoparticles for enhanced anti-tumor activities and hepatoprotection—synthesis, characterization and in vitro evaluation. J Nutr Biochem 26(11):1283–1297

[20] Sathishkumar M, Pavagadhi S, Mahadevan A, Balasubramanian R (2015) Biosynthesis of gold nanoparticles and related cytotoxicity evaluation using A549 cells. Ecotoxicol Environ Saf 114:232–240

[21] Murphy P, LaGrange M (1998) Raman spectroscopy of gold chloro-hydroxy speciation in fluids at ambient temperature and pressure: a re-evaluation of the effects of pH and chloride concentration. Geochim Cosmochim Acta 62(21):3515–3526

[22] Sathishkumar M, Mahadevan A, Vijayaraghavan K, Pavagadhi S, Balasubramanian R (2010) Green recovery of gold through biosorption, biocrystallization, and pyro-crystallization. Ind Eng Chem Res 49(16):7129–7135

[23] Naczk M, Shahidi F (2007) Corrigendum to "Phenolics in cereals, fruits and vegetables: occurrence, extraction and analysis". J Pharm Biomed Anal 43(2):798 **[(2006) J Pharm Biomed Anal 41:1523–1542]**

[24] Sneha K, Sathishkumar M, Kim S, Yun Y-S (2010) Counter ions and temperature incorporated tailoring of biogenic gold nanoparticles. Process Biochem 45(9):1450–1458

[25] Xin Lee K, Shameli K, Miyake M, Kuwano N, Bt Ahmad Khairudin NB, Bt Mohamad SE, Yew YP (2016) Green synthesis of gold nanoparticles using aqueous extract of *Garcinia mangostana* fruit peels. J Nanomater 2016:7

[26] Shahzadi P, Muhammad A, Mehmood F, Chaudhry MY (2014) Synthesis of 3, 7-dimethyl-2, 6-octadienal acetals from citral extracted from lemon grass, *Cymbopogon citrates* L. J Antivir Antiretrovir 2014:028–031

[27] Baker S, Satish S (2015) Biosynthesis of gold nanoparticles by *Pseudomonas veronii* AS41G inhabiting *Annona squamosa* L, Spectrochim. Acta A 150:691–695

[28] Mishra P, Ray S, Sinha S, Das B, Khan MI, Behera SK, Yun S-I, Tripathy SK, Mishra A (2016) Facile bio-synthesis of gold nanoparticles by using extract of *Hibiscus sabdariffa* and evaluation of its cytotoxicity against U87 glioblastoma cells under hyperglycemic condition. Biochem Eng J 105:264–272

[29] Ajitha B, Reddy YAK, Reddy PS (2015) Green synthesis and characterization of silver nanoparticles using *Lantana camara* leaf extract. Mater Sci Eng C 49:373–381

[30] Khandanlou R, Ngoh GC, Chong WT, Bayat S, Saki E (2016) Fabrication of silver nanoparticles supported on rice straw. In vitro antibacterial activity and its heterogeneous catalysis in the degradation of 4-nitrophenol. BioResources 11(2):3691–3708

[31] Levard C, Hotze EM, Lowry GV, Brown GE Jr (2012) Environmental transformations of silver nanoparticles: impact on stability and toxicity. Environ Sci Technol 46(13):6900–6914

[32] Karakoçak BB, Raliya R, Davis JT, Chavalmane S, Wang W-N, Ravi N, Biswas P (2016) Biocompatibility of gold nanoparticles in retinal pigment epithelial cell line. Toxicol In Vitro 37:61–69

[33] Stolarczyk EU, Stolarczyk K, Łaszcz M, Kubiszewski M, Maruszak W, Olejarz W, Bryk D (2017) Synthesis and characterization of genistein conjugated with gold nanoparticles and the study of their cytotoxic properties. Eur J Pharm Sci 96:176–185

[34] Konczak I, Zabaras D, Dunstan M, Aguas P (2010) Antioxidant capacity and phenolic compounds in commercially grown native Australian herbs and spices. Food Chem 122(1):260–266

[35] Rupesinghe EJR, Jones A, Shalliker RA, Pravadali-Cekic S (2016) A rapid screening analysis of antioxidant compounds in native australian food plants using multiplexed detection with active flow technology columns. Molecules 21(1):118

[36] Mata R, Nakkala JR, Sadras SR (2016) Polyphenol stabilized colloidal gold nanoparticles from *Abutilon indicum* leaf extract induce apoptosis in HT-29 colon cancer cells. Colloids Surf B 143:499–510

[37] Nirmala JG, Akila S, Narendhirakannan R, Chatterjee S (2017) Vitis vinifera peel polyphenols stabilized gold nanoparticles induce cytotoxicity and apoptotic cell death in A431 skin cancer cell lines. Adv Powder Technol 28:1170–1184

[38] Patra HK, Banerjee S, Chaudhuri U, Lahiri P, Dasgupta AK (2007) Cell selective response to gold nanoparticles. Nanomed Nanotech Biol Med 3(2):111–119

[39] Connor EE, Mwamuka J, Gole A, Murphy CJ, Wyatt MD (2005) Gold nanoparticles are taken up by human cells but do not cause acute cytotoxicity. Small 1(3):325–327

[40] Alkilany AM, Nagaria PK, Hexel CR, Shaw TJ, Murphy CJ, Wyatt MD (2009) Cellular uptake and cytotoxicity of gold nanorods: molecular origin of cytotoxicity and surface effects. Small 5(6):701–708

[41] Chithrani BD, Ghazani AA, Chan WC (2006) Determining the size and shape dependence of gold nanoparticle uptake into mammalian cells. Nano Lett 6(4):662–668

[42] AshaRani P, Low Kah Mun G, Hande MP, Valiyaveettil S (2008) Cytotoxicity and genotoxicity of silver nanoparticles in human cells. ACS Nano 3(2):279–290

[43] Kroemer G (1995) The pharmacology of T cell apoptosis. Adv Immunol 58:211–296

[44] Kumar R, Dwivedi PD, Dhawan A, Das M, Ansari KM (2011) Citrinin-generated reactive oxygen species cause cell cycle arrest leading to apoptosis via the intrinsic mitochondrial pathway in mouse skin. Toxicol Sci 122(2):557–566

[45] Nagajyothi P, Muthuraman P, Sreekanth T, Kim DH, Shim J (2016) Green synthesis: in-vitro anticancer activity of copper oxide nanoparticles against human cervical carcinoma cells. Arab J Chem 10:215–225

[46] Alkilany AM, Murphy CJ (2010) Toxicity and cellular uptake of gold nanoparticles: What we have learned so far? J Nanopart Res 12(7):2313–2333

[47] Arvizo R, Bhattacharya R, Mukherjee P (2010) Gold nanoparticles: opportunities and challenges in nanomedicine. Expert Opin Drug Deliv 7(6):753–763

[48] Sonavane G, Tomoda K, Makino K (2008) Biodistribution of colloidal gold nanoparticles after intravenous administration: effect of particle size. Colloid Surf B 66(2):274–280

[49] Chen Y-S, Hung Y-C, Liau I, Huang GS (2009) Assessment of the in vivo toxicity of gold nanoparticles. Nanoscale Res Lett 4(8):858

[50] Cho W-S, Cho M, Jeong J, Choi M, Cho H-Y, Han BS, Kim SH, Kim HO, Lim YT, Chung BH (2009) Acute toxicity and pharmacokinetics of 13 nm-sized PEG-coated gold nanoparticles. Toxicol Appl Pharmacol 236(1):16–24

[51] Dobrovolskaia MA, Patri AK, Zheng J, Clogston JD, Ayub N, Aggarwal P, Neun BW, Hall JB, McNeil SE (2009) Interaction of colloidal gold nanoparticles with human blood: effects on particle size and analysis of plasma protein binding profiles. Nanomed Nanotech Biol Med 5(2):106–117